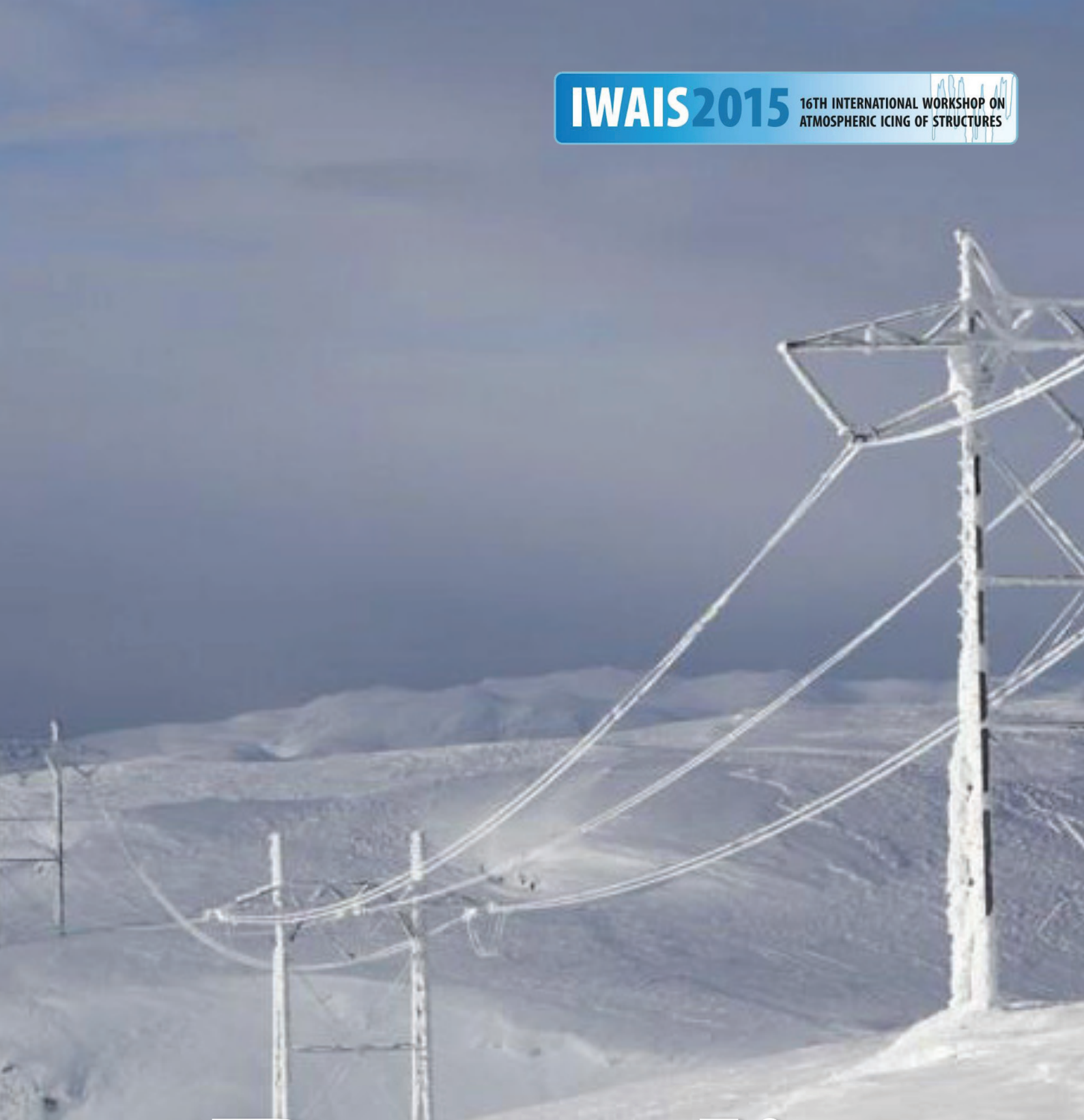

IWAIS2015 16TH INTERNATIONAL WORKSHOP ON ATMOSPHERIC ICING OF STRUCTURES

Proceedings

International Workshop on Atmospheric Icing of Structure

Swedish Energy Agency

Essential support for IWAIS 2015 has been provided by the Swedish Energy Agency

ISSN 2413-4597
ISBN 978-91-637-8552-8

ISSN 2413-4597
ISBN 978-91-637-8552-8

Passive acoustic signal sensing approach to detection of ice on the rotor blades of wind turbines

Eugen Mamontov [1], Viktor Berbyuk [2]
[1] Department of Research and Development, Foundation Chalmers Industrial Technology,
SE-412 88 Gothenburg, Sweden,
[2] Department of Applied Mechanics, Chalmers University of Technology
SE-412 96 Gothenburg, Sweden
eugen.mamontov@cit.chalmers.se

***Abstract*: In cold seasons, irregular layers of atmospheric ice (AI) are usually accreted on the rotor blades of operating wind turbines. For smart, energy-efficient deicing, ice-detection systems should not only detect the AI-layer on the blade skin (BS) but also provide the "landscape" of the material parameters of this layer over the BS surface, which generally vary in time. The work considers a passive sensing with wireless lowpass single-axis accelerometers, which are located at the centers of the mutually non-intersecting low-curvature disk-shape regions on the inner surface of the BS and measure acoustic accelerations normal to the surface. They include the acoustic component caused by the operational load in the BS. The work deals with this component only, and develops acoustic model and method for identification of the AI-layer parameters. The model is based on the third-order acoustic PDEs originating from the derived acoustic partial integro-differential equation, which includes the Boltzmann superposition integral with the related stress-relaxation function. The method can identify the following eight parameters: the thickness, volumetric mass density, bulk and shear moduli, stress-relaxation time, porosity, as well as volume and shear viscosities. The identification method is computationally efficient and can be suitable for implementation in the real-time mode. The proposed identification model and method enrich the scope of structural health monitoring of systems with the identification of material parameters of the thin-layer components. The work also suggests a few directions for future research.**

Keywords: blade of the operating wind turbine rotor, atmosheric ice, ice detection for smart deicing, third-order acoustic partial differential equation, parameter identification

Legend and Abbreviations

AI	*Atmosheric Ice*
IDS	*Ice-Detection System*
BS	*Blade Skin*
SRT	*Stress-Relaxation Time*
NEC	*Non-Equilibrium Component*
ANS	*Average Normal Stress*
TPD	*Thin Planar Disk*
PC	*Personal Computer*
FD	*Finite Difference*
PDE	*Partial Differential Equation*
SRF	*Stress-Relaxation Function*
ODE	*Ordinary Differential Equation*

Introduction

In cold seasons, irregular layers of atmospheric ice (AI) are usually accreted on the outer surfaces of the wind turbine rotor blades. These layers can cause unexpected down times and increase the maintenance cost, thereby reducing the energy-production efficiency. AI presents an unpredictable mixture of crystalline and amorphous ice including such forms as dense snow frozen to the surface, soft rime, hard rime, clear ice, and glaze (e.g., [1], [2]). The parameters of the AI-layer (e.g., the thickness, mass volumetric density, porosity, elastic moduli, viscosities, and stress-relaxation time) vary from a half on order to a few orders depending on the parameter (e.g., [3]–[5]).

For smart, energy-efficient deicing, ice-detection systems (IDSs) should not only detect the AI-layer on the blade skin (BS) but also provide the "landscape" of the material parameters of this layer over the BS surface, which generally vary in time. Consequently, the IDS development should deal with the following main features.

(1) The operational load in a BS creates irregular space-time distributions of material variables (e.g., strain, stress, and displacement) which depend on the acceleration, deceleration, speed of rotation of the rotor, the blade-pitch angle, the wind, the presence of the AI layer on the skin, and other factors. The corresponding experimental data are well documented (e.g., [6, Figs. 6–9], [7, Fig. 8 and Fig. 10(b)]).
(2) The BS-layer is of a complex, curvilinear shape that, in the course of the rotor operation, varies in space and time. This feature is also well documented (e.g., [6], [7]).
(3) The AI stress-relaxation time (STR) can be in an interval of a few orders (e.g., [3]–[5]).
(4) The aforementioned time-varying "landscape" of the AI-layer parameters should be identified with an appropriate acoustic model from the results measured by the IDS sensors, which are located on the inner BS surface and wirelessly controlled by a computer and gateways in the real-time mode.

Thus, the model and identification method are in the focus of the IDS development. The present work proposes acoustic model and method for identification the AI-layer parameters. The method uses the results of [8] and can estimate the following eight parameters: the thickness, mass density, bulk and shear moduli, STR, porosity, and volume and shear viscosities.

Due to the above Point (1), the identification method presumes passive rather than active sensing. The method is based on measurements of the acoustic accelerations at different points on the inner surface of the skin. (The acoustic acceleration is understood as, loosely speaking, the difference between

the total acceleration and the acceleration of the macroscopic motion.) The challenge in Point (2) is met by the extending the thin-planar-disk approximation introduced in [8] from a single solid layer to the two-layer sys-tem of the BS/AI layers. The features in the above Points (3) and (4) are allowed for by the corresponding generalization of the viscoelastic model developed in [8] and preceded in [9]. The model is based on a partial integro-differential equation for the non-equilibrium component (NEC) of the average normal stress (ANS) derived in [8, Sections 2 and 3]. The proposed identification method is computationally efficient and suitable for the use indicated in Point (4).

1. Acoustic model for the BS/AI-layer system

The model developed in [8] and generalized below is based on the thin-planar-disk (TPD) approximation, which is introduced in [8, Section 3] for the case of a single layer. This approximation presumes that:

- a major part of the space-time varying curvilinear skin of the operating blade with the AI layer accreted on its outer surface can be approximated with a set of mutually non-intersecting planar disk-shaped cylinders, briefly, disks;
- in each disk, the thicknesses of the BS- and AI-layers h_s and h are independent of the location on the disk surface;
- each disk is thin in the sense that

$$[(h_s+h)/R]^2 << 1 \qquad (1.1)$$

where R is the radius of the disk. Thus, the radiuses of all disks should be sufficiently small in order to allow the above planar-disk approximation and sufficiently big in order to enable inequality (1.1) for each disk to hold.

At the center of each disk on the inner surface of the BS layer, one attaches a wireless lowpass single-axis acoustic accelerometer measures the acoustic acceleration, which is normal to the surface. This acceleration is caused by the operational load in the layer. The accelerometer network can wirelessly be controlled by a personal computer (PC) and a gateway in the real-time mode. For better energy efficiency, this network should be endowed with wireless acoustic energy harvesters. The time developments of the accelerations measured at the point of the accelerometer locations are transmitted to the PC where the acoustic accelerations form the time-varying "landscape" of the data over the entire part of the two-layer-system surface represented with the TPD approximation. The PC by means of the acoustic model and identification method described below transforms these data into the space-time heterogeneous values of the AI-layer parameters

The model and method are the same for each disk. They apply the input data listed in Table 1.1.

Remark 1.1. As is well known, physical quantities at equilibrium are independent of time. The present work only considers materials, which are at equilibrium also independent of space. The equilibrium versions are denoted with the sign "overline" applied to the notation of the corresponding quantity (e.g., see the related notations in Table 1.1). □

As is shown in [8, Section 3], the above TPD approximation allows reduction of the model for a thin planar disk in three spatial dimension to the model in one spatial dimension, along the axis perpendicular to the disk, say, the x-axis. Without a loss of generality, one can consider that the inner surface of the BS-layer corresponds to value $x = 0$ and the x-axis has the origin at the center of the disk. Then the single-layer model of work [8] in the present case of the two-layer system can be written as the third-order partial differential equations (PDEs)

$$\bar{\theta}_s \partial^3\Pi_s/\partial t^3 + \partial^2\Pi_s/\partial t^2 = \bar{s}_s^2\left[\partial^2\Pi_s/\partial x^2 + 2\bar{\theta}_s\partial(\partial^2\Pi_s/\partial x^2)/\partial t\right], \quad 0 \le x \le h_s, \qquad (1.2)$$

$$\bar{\theta}\,\partial^3\Pi/\partial t^3 + \partial^2\Pi/\partial t^2 = \bar{s}^2\left[\partial^2\Pi/\partial x^2 + 2\bar{\theta}\,\partial(\partial^2\Pi/\partial x^2)/\partial t\right], \quad h_s \le x \le h_s + h, \qquad (1.3)$$

with boundary conditions

$$\Pi_s(0,t) = 0, \qquad (1.4)$$

$$\Pi_s(h_s,t) = \Pi(h_s,t), \qquad (1.5)$$

$$-\bar{\rho}_s^{-1}\,\partial\Pi_s(h_s,t)/\partial x = -\bar{\rho}^{-1}\,\partial\Pi(h_s,t)/\partial x, \qquad (1.6)$$

$$\Pi(h_s+h,t) = 0, \qquad (1.7)$$

and expression

$$a(t) = -\bar{\rho}_s^{-1}\,\partial\Delta\Pi_s(0,t)/\partial x \qquad (1.8)$$

for acoustic acceleration $a(t)$ (cp., Row 11 in Table 1.1). In the above relations, $\Pi_s = \Pi_s(x,t)$ and $\Pi = \Pi(x,t)$ are the NECs of the ANS in the BS and AI layers, h, $\bar{\rho}$, and $\bar{K}$ are the thickness, volumetric mass density, and bulk modulus of the AI layer, $\bar{\theta}_s$ and $\bar{\theta}$ are the SRTs of the BS and AI layers, and parameters

$$\bar{s}_s = \sqrt{\bar{K}_s/\bar{\rho}_s}, \qquad \bar{s} = \sqrt{\bar{K}/\bar{\rho}} \qquad (1.9)$$

are the speeds of the bulk acoustic waves in these layers. Inequality

$$\bar{\rho} > 0 \qquad (1.10)$$

holds because AI or, if it is absent, air, is not a vacuum. Note that the bulk waves in a medium are understood in the present

Table 1.1. The input data for the model and method for each disk in the TPD approximation.

The characteristics in Rows 2–8 and 11 generally dependent on the parameter in Row 1. The characteristics in Rows 1–8 are the same for each disk. They are assumed to be independent of time in each interval comprising any three successive time points (see Row 9). The data in Rows 9 and 10 can be specific to each disk. The data in Row 11 are specific to each disk.

	Notation	Meaning
1	$\bar{T}$	absolute temperature of AI
2	$\bar{\rho}_a$	volumetric mass density of air (used as described in Remark 1.2); it is 1.2 kg / m^3 at sea level
3	$\bar{\rho}_i$	volumetric mass density of a continuous, non-porous AI (used as described in Remark 1.2); it is 916.7 kg / m^3 at zero °C
4	h_s	thickness of the BS layer
5	$\bar{\rho}_s$	volumetric mass density of the BS
6	$\bar{K}_s$	bulk modulus of the BS
7	$\bar{\theta}_s$	stress-relaxation time in the BS
8	$s^*(\bar{\rho})$	dependence of the speed of the bulk acoustic waves in the AI layer (e.g., see (1.14))
9	N	number of the successive time points, at which the acceleration was measured; $N \ge 4$; this inequality allows to evaluate the third-order time derivatives with the help of finite-difference (FD) formulas
10	$t_1,...,t_N$	successive time points, $t_1<...<t_N$, at which the acceleration values were measured
11	$a_1,...,a_N$	values of acoustic acceleration $a(t)$ at time points t_k, $k = 1,2,...,N$; value a_k is the one at time point t_k; values a_k , $k = 1,2,...,N$, correspond to the NEC of the *operational-load-caused* stress force in the BS layer normal to the inner surface of the layer (cp., (1.8))

work as the waves related to *uniform* compressions/rarefactions. Also note that scalar PDE (1.2) or (1.3) can be quantitatively adequate only if the material is isotropic and the ratio of its shear modulus to the bulk one is sufficiently small (or, equivalently, the corresponding Poisson coefficient is not very far from 0.5).

A necessary condition for the applicability of linear quasi-equilibrium continuum-mechanics models such as acoustic equations (1.2) and (1.3) are relations (e.g., [8, (2.3)])

$$|\Delta p_s|/\bar{K}_s << 1, \qquad |\Delta p|/\bar{K} << 1, \qquad (1.11)$$

respectively, where Δp_s and Δp is the NECs of the pressures, which correspond to Π_s and Π, respectively, and are coupled with the latter by relations [8, (2.15)]

$$\Delta p_s = \Pi_s - \bar{\theta}_s \partial \Pi_s/\partial t - 2\bar{\theta}_s^2 \partial^2 \Pi_s/\partial t^2 + 4\bar{\theta}_s^2 \bar{s}_s^2 \partial^2 \Pi_s/\partial x^2. \qquad (1.12)$$

$$\Delta p = \Pi - \bar{\theta}\, \partial \Pi/\partial t - 2\bar{\theta}^2 \partial^2 \Pi/\partial t^2 + 4\bar{\theta}^2 \bar{s}^2 \partial^2 \Pi/\partial x^2. \qquad (1.13)$$

Expressions (1.12), (1.13), and inequalities (1.11) endow PDEs (1.2) and (1.3) with the self-testing capabilities [8, pp. 5-6].

It is shown in [8, Section 2] that, in PDE (1.2) (or (1.3)), the first term on the left-hand side and the multiplier "2" instead of "1" on the right-hand side result from the stress-relaxation function (SRF) in the Boltzmann superposition integral included in a more general, partial integro-differential equation derived in [8] (see [8, (2.10)]). The present forms of these terms correspond to the simplest, exponential approximation for the SRF.

Equation (1.2) and boundary conditions (1.4)–(1.6) form the boundary-value problem for the BS layer. Equation (1.3) and boundary conditions (1.5)–(1.7) form the boundary-value problem for the AI layer. These problems are mutually coupled because of the coupling of the layers with (1.5) and (1.6). Thus, (1.2)–(1.7) present a system of boundary-value problems. The solution of this system is the steady-state one because the operational load is long-lasting or, in modeling terms, defined in the entire time axis. Note that a steady-state solution of an asymptotically stable ordinary differential equation (ODE) in Euclidian space or a function Banach space is, loosely speaking, its unique solution with an initial condition in the limit case as the initial time point tends to $-\infty$ (e.g., see [11] for the details). This solution is specified with function $a(t)$ in (1.8).

Remark 1.2. If the AI-layer parameters $\bar{\rho}$, $\bar{K}$, and $\bar{\theta}$ are available, then the layer porosity $\bar{\varphi}$ ($0 \le \bar{\varphi} \le 1$), volume viscosity $\bar{\eta}$, shear modulus $\bar{G}$, and shear viscosity $\bar{\mu}$ can be estimated as $\bar{\varphi} = (\bar{\rho}_i - \bar{\rho})/(\bar{\rho}_i - \bar{\rho}_a)$, $\bar{\eta} = \bar{K}\bar{\theta}$, $\bar{G} = [s_T^*(\bar{\rho})]^2 \bar{\rho}$, and $\bar{\mu} = \bar{G}\bar{\theta}$, respectively, where $s_T^*(\bar{\rho})$ is the $\bar{\rho}$-dependence of the speed of the transverse acoustic waves in the AI layer. The speed of the longitudinal acoustic waves in the AI layer, $s_L^*(\bar{\rho})$, as a function of $\bar{\rho}$, can also be available. An experimental example of both the dependences for dense snow (including AI) can be found in [1, Fig. 2]. These data are related to the values of $\bar{\rho}$ in the entire dense-snow interval, i.e. from 300 kg/m^3 up to the value in Row 3 of Table 1.1. Functions $s_L^*(\cdot)$ and $s_T^*(\cdot)$ enable one to describe $s^*(\cdot)$ in Row 8 of Table 1.1. Indeed, due to (e.g., [10, (2.12), (2.14)])

$$s^*(\bar{\rho}) = \sqrt{[s_L^*(\bar{\rho})]^2 - (4/3)[s_T^*(\bar{\rho})]^2}. \qquad (1.14)$$

The aforementioned value $\bar{s}$ can be determined as

$$\bar{s} = s^*(\bar{\rho}) \qquad (1.15)$$

in terms of function (1.14). □

In view of Remark 1.2, the rest of the present work concentrates on identification of parameters h, $\bar{\rho}$, $\bar{K}$, and $\bar{\theta}$. This is carried out on the basis of boundary-value problem (1.2)–(1.7) and relation (1.8).

2. Separation of the boundary-value problem for the BS layer from the one for the AI layer

The treatment of the above boundary-value problem can be simplified if one separates the BS-layer subproblem from the AI-layer subproblem. This can be achieved by the following change of variables

$$\Pi_s(x,t) = Y_s(x,t) - hW(t)\,x, \qquad 0 \le x \le h_s, \qquad (2.1)$$

$$\Pi(x,t) = Y(x,t) + h_s W(t)\,[x - (h_s + h)], \quad h_s \le x \le h_s + h, \qquad (2.2)$$

where $Y_s(x,t)$ and $Y(x,t)$ are the new variables, and

$$W(t) = (\bar{\rho}_s h_s + \bar{\rho}\, h)^{-1}\left[\bar{\rho}\, \partial Y_s(h_s,t)/\partial x - \bar{\rho}_s\, \partial Y(h_s,t)/\partial x\right] \qquad (2.3)$$

is an auxiliary function. Boundary conditions (1.4)–(1.7) for Π_s and Π correspond to zero boundary conditions for Y_s and Y,

$$Y_s(0,t) = Y_s(h_s,t) = 0, \qquad (2.4)$$

$$Y(h_s,t) = Y(h_s + h,t) = 0. \qquad (2.5)$$

In view of (1.8) and (2.1),

$$h\,W(t) = f_0(t) \qquad (2.6)$$

where

$$f_0(t) = \bar{\rho}_s\, a(t) + \partial Y_s(0,t)/\partial x. \qquad (2.7)$$

In the limit case as the AI-layer thickness h tends to zero, limit relation

$$\lim_{h \downarrow 0} f_0(t) = 0 \qquad (2.8)$$

holds because of (2.1), (2.3), and (2.6).

Importantly, relations (2.3) and (2.6) enables one to express a certain characteristic of the AI layer in terms of the related characteristics of the skin layer, namely

$$\bar{\rho}_s h \frac{\partial Y(h_s,t)}{\partial x} = \bar{\rho}\, h \frac{\partial Y_s(h_s,t)}{\partial x} - (\bar{\rho}_s h_s + \bar{\rho}\, h) f_0(t)$$
$$= -\bar{\rho}_s h_s f_0(t) + \bar{\rho}\, h f_1(t) \qquad (2.9)$$

where

$$f_1(t) = \partial Y_s(h_s,t)/\partial x - f_0(t). \qquad (2.10)$$

Application of (2.1) and (2.2) to PDEs (1.2) and (1.3), as well as allowing for (2.6) lead to the BS and AI-layer PDEs

$$\bar{\theta}_s \frac{\partial^3 Y_s}{\partial t^3} + \frac{\partial^2 Y_s}{\partial t^2} = \bar{s}_s^2 \left(\frac{\partial^2 Y_s}{\partial x^2} + 2\bar{\theta}_s \frac{\partial}{\partial t} \frac{\partial^2 Y_s}{\partial x^2} \right)$$
$$+ \left[\bar{\theta}_s \frac{d^3 f_0(t)}{dt^3} + \frac{d^2 f_0(t)}{dt^2} \right] x, \qquad 0 \le x \le h_s, \qquad (2.11)$$

$$\bar{\theta} \frac{\partial^3 Y}{\partial t^3} + \frac{\partial^2 Y}{\partial t^2} = \bar{s}^2 \left(\frac{\partial^2 Y}{\partial x^2} + 2\bar{\theta} \frac{\partial}{\partial t} \frac{\partial^2 Y}{\partial x^2} \right)$$
$$- \frac{h_s}{h} \left[\bar{\theta} \frac{d^3 f_0(t)}{dt^3} + \frac{d^2 f_0(t)}{dt^2} \right] [x - (h_s + h)], \quad h_s \le x \le h_s + h. \qquad (2.12)$$

One can see that the change of variables (2.1), (2.2) allows achieving the separation of the BS-layer boundary-value problem from the AI-layer. Indeed, in terms of new variables Y_s and Y, the BS-layer boundary-value problem (2.11), (2.7), (2.4) is independent of the AY-layer boundary-value problem (2.12), (2.7), (2.5).

Consequently, one can first reconstruct the solution of the first problem by using already known function $a(t)$ in (2.7), and then apply this function and the obtained solution to determine the solution of the second problem, which will allow to regard equation (2.12) as the equation for identification of the parameters h, $\bar{\rho}$, $\bar{K}$, and $\bar{\theta}$.

The first and second parts of this program are considered in Sections 3 and 4. The latter one uses the following three equations related to (2.12). In view of (2.1), the versions of PDE (2.12) at $x = h_s$ and $x = h_s + h$ are

$$\bar{s}^2\left\{\partial^2 Y(h_s,t)/\partial x^2 + 2\bar{\theta}\, d\,[\partial^2 Y(h_s,t)/\partial x^2]/dt\right\} + h_s\left[\bar{\theta}\, d^3 f_0(t)/dt^3 + d^2 f_0(t)/dt^2\right] = 0, \quad (2.13)$$

$$\bar{s}^2\left[\partial^2 Y(h_s+h,t)/\partial x^2 + 2\bar{\theta}\, d\,[\partial^2 Y(h_s+h,t)/\partial x^2]/dt\right] = 0. \quad (2.14)$$

Also, differentiating (2.12) with respect to x and substituting value $x = h_s$ into the resulting equality, one obtains equation

$$\bar{\theta}\frac{d^3}{dt^3}\frac{\partial Y(h_s,t)}{\partial x} + \frac{d^2}{dt^2}\frac{\partial Y(h_s,t)}{\partial x} = \bar{s}^2\left[\frac{\partial^3 Y(h_s,t)}{\partial x^3} + 2\bar{\theta}\frac{d}{dt}\frac{\partial^3 Y(h_s,t)}{\partial x^3}\right] - \frac{h_s}{h}\left[\bar{\theta}\frac{d^3 f_0(t)}{dt^3} + \frac{d^2 f_0(t)}{dt^2}\right].$$

Multiplication of it by $\bar{\rho}_s h$ and substitution of (2.9) into the left-hand side of the resulting equality lead to

$$\bar{\rho}\left[\bar{\theta}\frac{d^3 f_1(t)}{dt^3} + \frac{d^2 f_1(t)}{dt^2}\right] = \bar{\rho}_s \bar{s}^2\left[\frac{\partial^3 Y(h_s,t)}{\partial x^3} + 2\bar{\theta}\frac{d}{dt}\frac{\partial^3 Y(h_s,t)}{\partial x^3}\right], \quad h > 0. \quad (2.15)$$

By introducing an appropriate approximation for the term in the brackets on the right-hand side of (2.15), one can obtain a time-varying algebraic equation for parameters to be identified, i.e., h, $\bar{\rho}$, $\bar{K}$, and $\bar{\theta}$. This is considered in Section 4.

3. Reconstruction of the Steady-State Solution of the Boundary-Value Problem for the BS-Layer

Change of variables (2.1), (2.2) not only allows the separation discussed in Section 2 but also provides homogeneous boundary conditions (2.4), (2.5). Relations (2.4) enables one to reconstruct the solution of the BS-layer boundary-value problem (2.11), (2.7), (2.4) by means of the Fourier method (e.g., [12, Chapters VIII and IX]). It provides expansions of solutions of linear PDEs, which are based on the Laplace operator, in the operator eigenfunctions (e.g., [13, Chapter V]).

The Laplace operator in the BS-layer PDE (2.11) is differential expression $\partial^2/\partial x^2$ endowed with boundary conditions (2.4). The eigenvalues and eigenfunctions for this operator are well known (e.g., [12, pp. 118-119], [13, Chapter V, Section 22.4, (21)]. The eigenvalues are $-\kappa_{s.i}^2$, $i = 1,2,\ldots$, where

$$\kappa_{s.i} = (\pi/h_s)\, i, \qquad i = 1,2,\ldots, \quad (3.1)$$

and the orthonormal eigenfunctions are

$$X_{s.i}(x) = \sqrt{2/h_s}\sin(\kappa_{s.i}x), \quad 0 \le x \le h_s, \quad i = 1,2,\ldots. \quad (3.2)$$

According to the Fourier method, solutions of boundary-value problem (2.11), (2.4) is presented in the form

$$Y_s(x,t) = \Sigma_{i=1}^{\infty}\Theta_{s.i}(t)X_{s.i}(x), \quad 0 \le x \le h_s, \quad (3.3)$$

where $\Theta_{s.i}(t)$ are the time-dependent coefficients of the expansion. Combining (3.1)–(3.3), one obtains

$$\partial Y_s(0,t)/\partial x = \sqrt{2/h_s}\,(\pi/h_s)\,\Sigma_{j=1}^{\infty} j\,\Theta_{s.j}(t), \quad (3.4)$$

$$\partial Y_s(h_s,t)/\partial x = \sqrt{2/h_s}\,(\pi/h_s)\,\Sigma_{j=1}^{\infty}(-1)^j j\,\Theta_{s.j}(t). \quad (3.5)$$

Since (2.11) includes the source function, which is linear and homogeneous in x, one also needs to consider the corresponding expansions for these functions. By using (3.1), (3.2), and the well-known results (e.g., [13, Sections 21.4 and 22.3 of Chapter V], [14, 430.11]), one can show that the expansions are the following:

$$x = \sum_{i=1}^{\infty}\left[\sqrt{2/h_s}\int_0^{h_s} x_*\sin(\kappa_{s.i}x_*)\,dx_*\right]\left[\sqrt{2/h_s}\sin(\kappa_{s.i}x)\right] = \sum_{i=1}^{\infty}\sqrt{2h_s}\,\frac{(-1)^{i-1}}{\kappa_{s.i}}\left[\sqrt{2/h_s}\sin(\kappa_{s.i}x)\right] = \sum_{i=1}^{\infty}\sqrt{2h_s}\,h_s\,\frac{(-1)^{i-1}}{\pi i}X_{s.i}(x), \quad 0 \le x \le h_s. \quad (3.6)$$

Remark 3.1. The terms in the series in (3.6) contribute to both the shape and integral over the corresponding x-interval of the function on the left-hand side. However, it appears that these contributions are qualitatively different.

In view of (3.2), the terms in (3.6) with odd and even values of i are even and odd functions of $x - h_s/2$, respectively. This means that the even terms substantially contribute to the correspondence of the shape of the x-dependence on the right-hand side of (3.6) to function x on the left-hand side.

Moreover, as follows from (3.6),

$$\int_0^{h_s} x\,dx = \frac{h_s^2}{2} = 2\sum_{i=1}^{\infty}\frac{(-1)^{i-1}}{\kappa_{s.i}}\int_0^{h_s}\sin(\kappa_{s.i}x)\,dx = \frac{h_s^2}{2}\,\frac{8}{\pi^2}\sum_{i=1}^{\infty}\frac{1-(-1)^i}{2}\,\frac{1}{i^2}. \quad (3.7)$$

The sum of the series on the right-hand side of (3.7) can be evaluated as follows (e.g., [14, (48.12)])

$$\Sigma_{i=1}^{\infty}[1-(-1)^i]/(2/i^2) = \pi^2/8. \quad (3.8)$$

Relations (3.7) and (3.8) show that the terms with even values of i do not contribute to the integral at all. They only, so to say, correct the shape of the approximation formed by the preceding terms of the series. This means that, if the series is approximated with the finite sum corresponding to the values of i from unit to, say, $J \ge 1$, it is reasonable to do that at even J.

One can also check that the integral can be approximated with a very small relative error, say, of 5% when at least eight terms of the series are taken into account. This indicates that J should be not only even but also not less than eight. □

Since PDE (2.11), by means of (2.7), involves not only $a(t)$ but also $\partial Y_s(0,t)/\partial x$, which a value of the solution of the BS-layer boundary-value problem, it is necessary to rewrite (2.11) in the corresponding form, i.e.,

$$\bar{\theta}_s\frac{\partial^3 Y_s}{\partial t^3} + \frac{\partial^2 Y_s}{\partial t^2} = \bar{s}_s^2\left[\frac{\partial^2 Y_s}{\partial x^2} + 2\bar{\theta}_s\frac{\partial}{\partial t}\left(\frac{\partial^2 Y_s}{\partial x^2}\right)\right] + \left\{\bar{\rho}_s\left[\bar{\theta}_s\frac{d^3 a(t)}{dt^3} + \frac{d^2 a(t)}{dt^2}\right] + \left[\bar{\theta}_s\frac{d^3}{dt^3}\frac{\partial Y_s(0,t)}{\partial x} + \frac{d^2}{dt^2}\frac{\partial Y_s(0,t)}{\partial x}\right]\right\}x, \quad 0 \le x \le h_s. \quad (3.9)$$

Substitution of (3.3), (3.4), and (3.6) into (3.9) results in

$$\bar{\theta}_s\left[\frac{d^3\Theta_{s.i}(t)}{dt^3} + \frac{(-1)^i 2}{i}\Sigma_{j=1}^{\infty} j\frac{d^3\Theta_{s.j}(t)}{dt^3}\right] + \left[\frac{d^2\Theta_{s.i}(t)}{dt^2} + \frac{(-1)^i 2}{i}\Sigma_{j=1}^{\infty} j\frac{d^2\Theta_{s.j}(t)}{dt^2}\right] + \bar{s}_s^2\frac{\pi^2}{h_s^2}i^2\left[\bar{\theta}_s\frac{d\Theta_{s.i}(t)}{dt} + \Theta_{s.i}(t)\right] = \frac{\bar{\rho}_s\sqrt{2h_s}\,h_s}{\pi}\,\frac{(-1)^{i-1}}{i}\left[\bar{\theta}_s\frac{d^3 a(t)}{dt^3} + \frac{d^2 a(t)}{dt^2}\right], \quad i = 1,2,\ldots. \quad (3.10)$$

Thus, coefficients $\Theta_{s.1}(t), \Theta_{s.2}(t), \ldots$ of the Fourier expansion (3.3) are described with infinite-dimensional ODE system (3.10). In practice, one can solve it in the finite-dimensional approximation. More specifically, at any $J \ge 1$, the Jth-approximation versions of (3.3)–(3.5) and (3.10) are

$$Y_s(x,t) = \Sigma_{i=1}^{J}\Theta_{s.i}(t)X_{s.i}(x), \qquad 0 \le x \le h_s, \quad (3.11)$$

$$\frac{\partial Y_s(0,t)}{\partial x} = \sqrt{\frac{2}{h_s}}\,\frac{\pi}{h_s}\,\Sigma_{j=1}^{J} j\,\Theta_{s.j}(t), \quad (3.12)$$

$$\frac{\partial Y_s(h_s,t)}{\partial x} = \sqrt{\frac{2}{h_s}}\,\frac{\pi}{h_s}\,\Sigma_{j=1}^{J}(-1)^j j\,\Theta_{s.j}(t), \quad (3.13)$$

$$\bar{\theta}_s\left[\frac{d^3\Theta_{s.i}(t)}{dt^3}+\frac{(-1)^i 2}{i}\sum_{j=1}^{J} j\,\frac{d^3\Theta_{s.j}(t)}{dt^3}\right]$$
$$+\left[\frac{d^2\Theta_{s.i}(t)}{dt^2}+\frac{(-1)^i 2}{i}\sum_{j=1}^{J} j\,\frac{d^2\Theta_{s.j}(t)}{dt^2}\right]$$
$$+\bar{s}_s^2\frac{\pi^2}{h_s^2}i^2\left[\bar{\theta}_s\frac{d\Theta_{s.i}(t)}{dt}+\Theta_{s.i}(t)\right]$$
$$=\frac{\bar{\rho}_s\sqrt{2h_s}h_s}{\pi}\frac{(-1)^{i-1}}{i}\left[\bar{\theta}_s\frac{d^3a(t)}{dt^3}+\frac{d^2a(t)}{dt^2}\right],\quad i=1,2,\ldots. \quad (3.14)$$

According to Remark 3.1, number J should be even and such that $J\geq 8$.

As follows from Table 1.1, acoustic acceleration $a(t)$ in (3.14) is available in the form of values $a_1, a_2, \ldots$ measured in a set of successive time points t_k, $k=1,\ldots,N$, $N\geq 4$. Accordingly, at each $i=1,\ldots,J$, one can consider values $\Theta_{s.i.k}$ of $\Theta_{s.i}(t)$ at the mentioned time points and express the time derivatives of functions $a(t)$ and $\Theta_{s.i}(t)$ by means of the corresponding FD formulas. This will result in the system of NJ linear algebraic equations with constant coefficients for NJ values $\Theta_{s.i.k}$, $i=1,\ldots,J$, $k=1,\ldots,N$. Assuming that the matrix of this system is nonsingular, one can uniquely solve the system for the mentioned values.

Remark 3.2. The output data of the above solution procedure are values $d^{(l)}f_0(t)/dt^{(l)}$ and $d^{(l)}f_1(t)/dt^{(l)}$, $l=0,1,2,3$, at points $t=t_k$, $k=1,\ldots,N$, which are evaluated as scalars $f_{0.k}^{(l)}$ and $f_{0.k}^{(l)}$ by means of (2.7), (2.10), measured acoustic-acceleration values a_k, expressions (3.12), (3.13), and the FD formulas based on the obtained values $\Theta_{s.i.k}$. □

Remark 3.2 is used in the method described below.

4. Equation and Method for Identification of the Four Parameters of the AI-Layer

Equality (2.15) can be used for identification of the AI-layer parameters h, $\bar{\rho}$, $\bar{s}$, and $\bar{\theta}$ provided that one estimates the term in the brackets on the right-hand side by means of available acoustic acceleration $a(t)$ or the parameters to be identified. In order to do that, one can apply the approach developed in [8, Section 4] for a single layer to the present case of the AI layer in the two-layer, skin/AI system.

According to this approach, it can be sufficient to approximate $Y(x,t)$ with the fourth-order polynomial

$$Y(x,t)\approx[b_2(t)(x-h_s)^2+b_1(t)(x-h_s)+b_0(t)][(x-h_s)^2-h(x-h_s)]$$
$$=b_2(t)(x-h_s)^4+[b_1(t)-b_2(t)h](x-h_s)^3$$
$$+[b_0(t)-b_1(t)h](x-h_s)^2-b_0(t)h(x-h_s),\quad h_s\leq x\leq h_s+h, \quad (4.1)$$

which has two t-independent roots $x=h_s$ and $x=h_s+h$ according to (2.5), and a pair of real or complex conjugate roots that need not be t-independent. In order to obtain the above estimation, one can involve relations (2.9), (2.13), and (2.14), and, thus, the x-derivatives of (4.1) of the first, second, and third orders. (The third-order derivative is used in (2.15).)

Differentiation of (4.1) three times in x and combining the obtained derivatives of the first, second, and third orders with relations (2.9), (2.13), and (2.14), one derives expression

$$\bar{s}^2\left\{\partial^3 Y(h_s,t)/\partial x^3+2\bar{\theta}\,d\left[\partial^3 Y(h_s,t)/\partial x^3\right]/dt\right\}$$
$$=(1/h)\left\{12(\bar{s}/h)^2\left[h_s[f_0(t)+2\bar{\theta}\,df_0(t)/dt]\right.\right.$$
$$\left.-(\bar{\rho}h/\bar{\rho}_s)[f_1(t)+2\bar{\theta}\,df_1(t)/dt]\right]$$
$$\left.+5h_s\left[\bar{\theta}\,d^3f_0(t)/dt^3+d^2f_0(t)/dt^2\right]\right\}. \quad (4.2)$$

Application of (4.2) to the right-hand side of (2.15) transforms the latter into

$$\bar{\rho}h\left[\bar{\theta}\,d^3f_1(t)/dt^3+d^2f_1(t)/dt^2\right]$$
$$+12(\bar{s}/h)^2\left[\bar{\rho}h[f_1(t)+2\bar{\theta}\,df_1(t)/dt]\right.$$
$$\left.-\bar{\rho}_s h_s[f_0(t)+2\bar{\theta}\,df_0(t)/dt]\right]$$
$$-5\bar{\rho}_s h_s\left[\bar{\theta}\,d^3f_0(t)/dt^3+d^2f_0(t)/dt^2\right]=0,\quad h>0, \quad (4.3)$$

This is the equation for identification of the AI-layer parameters h, $\bar{\rho}$, $\bar{s}$, and $\bar{\theta}$.

One can emphasize the different roles of terms $f_0(t)$ and $f_1(t)$ in (4.3) by moving the related terms to the right- and left-hand sides, respectively. This results in

$$\bar{\rho}h\left\{\bar{\theta}\,d^3f_1(t)/dt^3+d^2f_1(t)/dt^2+12(\bar{s}/h)^2[f_1(t)+2\bar{\theta}\,df_1(t)/dt]\right\}$$
$$=\bar{\rho}_s h_s\left\{5[\bar{\theta}\,d^3f_0(t)/dt^3+d^2f_0(t)/dt^2]\right.$$
$$\left.+12(\bar{s}/h)^2[f_0(t)+2\bar{\theta}\,df_0(t)/dt]\right\},\quad h>0, \quad (4.4)$$

The form of this relation, as well as notations (2.7) and (2.10) confirm that it is a relation for the two-layer system. Equation (4.4) is a generalization of a single-layer equation [8, (4.2)] obtained by means of the fourth-order-polynomial approximation (4.1) (or [8, (4.1)]). Indeed, equation (4.4) regarded as an ODE for $f_1(t)$ is analogous to the single-layer ODE [8, (4.2)]. The structure of the left-hand side of (4.4) coincides with the one of the left-hand side of [8, (4.2)]. However, in contrast to the single-layer ODE, which is homogeneous, the two-layer ODE (4.4) is nonhomogeneous: it is driven with the right-hand side determined by term $f_0(t)$.

The identification method based on equation (4.3) described below.

Dividing (4.3) by $\rho_s h_s$, one reduces it to the following more compact form

$$q\left[\bar{\theta}\,d^3f_1(t)/dt^3+d^2f_1(t)/dt^2\right]$$
$$-12c\left[[f_0(t)+2\bar{\theta}\,df_0(t)/dt]-q[f_1(t)+2\bar{\theta}\,df_1(t)/dt]\right]$$
$$-5\left[\bar{\theta}\,d^3f_0(t)/dt^3+d^2f_0(t)/dt^2\right]=0,\quad h>0, \quad (4.5)$$

where

$$c=(\bar{s}/h)^2>0, \quad (4.6)$$
$$q=(\bar{\rho}h)/(\bar{\rho}_s h_s)>0. \quad (4.7)$$

The inequalities in (4.6) and (4.7) follow from (1.10) and the inequality in (4.5). Equation (4.5) is the equation for identification of parameters $\bar{\theta}$, c, and q. The input data for (4.5) are the output data specified in Remark 3.2.

If parameters c and q are available, then parameters $\bar{\rho}$, $\bar{s}$, and h can be determined uniquely. Indeed, as follows from (4.6) and (4.7), $\bar{\rho}\bar{s}=(\bar{\rho}_s h_s)q\sqrt{c}$. Since $\bar{s}$ can be presented with dependence $\bar{s}^*(\bar{\rho})$ (see the text on (1.14) and Row 8 of Table 1.1), which is monotonically increasing, the indicated equality enables one to determine $\bar{\rho}$ as the unique solution of equation

$$\bar{\rho}\,\bar{s}^*(\bar{\rho})=(\bar{\rho}_s h_s)q\sqrt{c}. \quad (4.8)$$

As soon as $\bar{\rho}$ is available, $\bar{s}$ and h are calculated with (1.15) and (4.6) or (4.7), respectively. In turn, after the AI-layer parameters h, $\bar{\rho}$, $\bar{s}$, and $\bar{\theta}$ are identified, the other parameters of the layer can be determined in the way described in Remark 1.2.

Note that, as follows from the inequality in (4.5), the equation in (4.5) is applicable at any $h>0$. However, in view of notations (4.6), (4.7), and relation (2.8), the equation becomes an identity in the limit case as $h\downarrow 0$ and, thus, remains valid in this limit case as well.

The left-hand side of (4.5) is a polynomial of the degree not greater then three of three variables, parameters c, q, and $\bar{\theta}$. Thus, it is in general a tri-linear function, i.e., linear in each of the three variables. In general, the parameters can be identified

with the help of equation (4.5) in different ways. The simplest one is evaluation of them from the equation system consisting of the three versions of equation (4.5) at three successive time points, say, t_{k-2}, t_{k-1}, and t_k, $k=3,...,N$, where, in each version, the time derivatives are replaced with the FD formulas mentioned in Remark 3.2. This presumes that parameters c, q, and $\bar{\theta}$ are t-independent in interval $[t_{k-2},t_k]$ and, thus, are represented with their values c_k, q_k, and $\bar{\theta}_k$ specific to this interval. These values are determined as the unique solution of the mentioned system of the three tri-linear equations. This solution is suitable only if (see (4.6) and (4.7)) $c_k>0$, $q_k>0$, and $\bar{\theta}_k \geq 0$. The determined values present the parameters identified in interval $[t_{k-2},t_k]$.

Applying this procedure to the intervals corresponding to each of $k=3,...,N$, one obtains the piecewise-constant t-dependent approximations for the identified AI-layer parameters. These t-dependences include the influence of the operational load upon the parameters.

In view of the approximate nature of the FD formulas used in the proposed method, the t-dependences can be rather irregular. Consequently, they, in general, need to be "smoothed" in order to provide the component, which is caused by the operational load rather than the quantitative FD errors. The "smoothing" method can be a topic for future research.

At each $k=3,...,N$, the coefficients of the corresponding system of three tri-linear equations completely determine many of the properties of the system, for instance, the following.

- Does it have at least one suitable (see above) solution?
- If yes, how many solutions of this type exist?
- If more than one, how can one choose the most suitable?

These questions also present topics for future study. Some of them can be contributed with practical methods. Tri-linear systems are nonlinear. They can be solved with direct, non-iterative techniques or iterative techniques. Direct methods are not often applied to nonlinear systems because the corresponding analytical treatments are available in exceptional cases only. For this reason, it is much easier to use iterative methods. Book [15] provides a comprehensive introduction in this field.

However, iterative methods are difficult to use in the real-time computing because of at least two still unanswered questions.

- How can one assure unquestionable convergence of the iterations to a solution of the nonlinear system?
- How can one choose the initial approximation such that the resulting iterative approximations converge to the solution of interest?

The related difficulties usually presume intervention of an expert (e.g., a user) in the computational process. But these interventions are inappropriate to the real-time mode. Due to that, one can more closely consider direct methods. For example, one of them can be based on the procedure similar the one described in [8, the text on (4.5) and (4.6)]. The resulting identification can be computationally efficient and relevant for implementation in the real-time mode.

One more topic for future research is a calibration of the proposed identification method with respect to the related experimental data.

5. Conclusion

The present work generalizes the approach to a thin single solid layer (documented in one of the previous papers of the authors) for the case of a thin two-layer system, which comprises the BS and AI layers. They are assumed to be isotropic and isothermal. The work considers a passive sensing with wireless lowpass single-axis acoustic accelerometers, which are located at the centers of the mutually non-intersecting low-curvature disk-shape regions on the inner surface of the BS and measure acoustic accelerations, which are normal to the surface and caused by the operational load in the BS. The work develops the acoustic model based on the third-order PDE and the resulting from it method for identification of the following eight parameters of the AI-layer: the thickness, volumetric mass density, bulk and shear moduli, SRT, porosity, and volume and shear viscosities. The identification method is computationally efficient and can be suitable for implementation in the real-time mode. The proposed identification model and method enrich the scope of structural health monitoring of systems with the identification of material parameters of the thin-layer components. The work also suggests a few directions for future research.

Acknowledgement

The authors thank the Swedish Energy Agency for a partial support of the present work via the project 37286-1.

References

[1] R.A. Sommerfeld, "A review of snow acoustics", Rev. Geophys. & Space Phys., 20(1), 1982, 62-66.

[2] H. Gao, J.L. Rose, "Ice detection and classification on an aircraft wing with ultrasonic shear horizontal guided waves", IEEE Trans. Ultrasonics, Ferroelectrics, & Frequency Control, 56(2), 2009, 334-344.

[3] b. R.M. Deeley, "The viscosity of ice", Proc. Royal Soc. London. Series A 81(547; Sep. 11), 1908, 250-259.

[4] P.P. Kobeko *et al.*, "Plastic deformation and viscosity of ice", J. Tech. Phys., 16(3), 1946, 263-272.

[5] P.V. Hobbs, Ice Physics, Clarendon Press, Oxford, 1974.

[6] K. Schroeder *et al.*, "A fibre Bragg grating sensor system monitors operational load in a wind turbine rotor blade", Meas. Sci. Technol. 17, 2006, 1167–1172.

[7] J.R. White *et al.*, "Operational load estimation of a smart wind turbine rotor blade", Proc. of SPIE 7295, 2009, 72952D/1-72952D/12.

[8] E. Mamontov, V. Berbyuk, "Identification of material parameters of thin curvilinear viscoelastic solid layers in ships and ocean structures by sensing the bulk acoustic signals", VI Int. Conf. Comput. Meth. Marine Engrng, MARINE 2015, (F. Salvatore, R. Broglia, and R. Muscari, Eds.) 15-17 June 2015, Rome, Italy, 12 pp.

[9] E. Mamontov, V. Berbyuk, "A scalar acoustic equation for gases, liquids, and solids, including viscoelastic media", J. Appl. Math. & Phys, 2, 2014, 960-970.

[10] H.F. Pollard, Sound Waves in Solids, Pion, London, 1977.

[11] E. Mamontov, "Dynamic-equilibrium solutions of ordinary differential equations and their role in applied problems", Appl. Math. Lett., 21(4), 2008, 320-325.

[12] N.S. Koshlyakov, M.M. Smirnov, E.B. Gliner, Differential Equations of Mathematical Physics, North-Holland Publishing, Amsterdam, 1964.

[13] V.S. Vladimirov, Equations of Mathematical Physics, Mir, Moscow, 1984.

[14] H.B. Dwight, Tables of integrals and other mathematical data, McMillan, New York, 1961.

[15] J.M. Ortega, W.R. Rheinboldt, Iterative Solution of Nonlinear Equations in Several Variables, Acad. Press, New York, 1970.